Journal of Alloys and Compounds 408–412 (2006) 1182–1186

Journal of ALLOYS AND COMPOUNDS

www.elsevier.com/locate/jallcom

Phase transition of $BaNd_2Mn_2O_7$

Jian Meng *, Hirohisa Satoh, Masahiro Ishida, Naoki Kamegashira

Department of Materials Science, Toyohashi University of Technology, Tempaku-cho, Toyohashi 441-8580, Japan

Received 30 July 2004; received in revised form 29 October 2004; accepted 15 December 2004
Available online 1 August 2005

Abstract

Phase transition of $BaNd_2Mn_2O_7$ from orthorhombic (space group *Fmmm*) to tetragonal phase (*I*4/*mmm*) was studied by high temperature powder X-ray diffractometry and Rietveld analysis. The transition temperature was identified at 523 K, which is almost the same transition temperature as the compounds with other rare earth ions in this $BaLn_2Mn_2O_7$ family (Ln = Sm and Eu) with *Fmmm* space group. During the transition an oxygen octahedron of each phase changes a little its form, in which four oxygen atoms perpendicular to *c*-axis make a rectangle and a square for orthorhombic and tetragonal phases, respectively. Manganese ion is not on the center of the quadrilateral consisting of these four oxygen ions, but a little apart from the center along *c*-axis in both phases.

Keywords: Phase transition; Barium neodymium manganese oxide ($BaNd_2Mn_2O_7$); High temperature X-ray diffractometry; Oxygen octahedron; Crystal structure and symmetry

1. Introduction

Layered perovskites $BaLn_2Mn_2O_7$ (Ln = lanthanide) which belong to a Ruddlesden–Popper-type homologous series $AO{\cdot}(ABO_3)_n$ with $n = 2$ [1] were synthesized by Deschizeaux-Cheruy and Joubert [2] for various rare earths. According to their results, these compounds fundamentally crystallize into a body centered tetragonal structure with the $Sr_3Ti_2O_7$-type for Ln = Pr–Gd but there is another phase with an orthorhombic distortion for Ln = Nd, Sm and Eu when these compounds were prepared in N_2 atmosphere. The existence of another type of orthorhombic phase for Ln = Tb [3] and Gd [4] are known. A clear difference between these two orthorhombic phases is seen in the X-ray powder diffraction patterns [5]. For example, the main peak is a single peak in an orthorhombic compound for Ln = Eu, Sm or Nd and the second one splits into double peaks with the lattice parameters $a_o \fallingdotseq b_o \fallingdotseq \sqrt{2}a_t$ and $c_o \fallingdotseq c_t$, where a_o, b_o and c_o are the lattice constants in the orthorhombic phase and a_t and c_t are those in the fundamental tetragonal phase. On the other hand, the reverted situation occurs in another type of orthorhombic compound for Ln = Gd and Tb with the lattice parameters $a_o \fallingdotseq b_o \fallingdotseq a_t$ and $c_o \fallingdotseq c_t$.

Each orthorhombic phase for Ln = Sm, Eu, Gd and Tb has phase transition to tetragonal one at high temperature which are characterized by several experimental results [3,6–16]. About $BaNd_2Mn_2O_7$ with the former distortion, the detailed crystal structure with *Fmmm* of the space group was studied by the present authors [17], but no information on the phase transition has been reported. This is because it is rather difficult to synthesize a single phase of these distorted phases, especially orthorhombic $BaNd_2Mn_2O_7$, since formation of these phases depends upon various synthetic conditions such as atmospheric oxygen partial pressure during the heating, cooling rate after preparation and other factors. This paper describes the results of high temperature X-ray diffractometry to observe the phase transition.

* Corresponding author. Present address: Key Laboratory of Rare Earth Chemistry and Physics, Changchun Institute of Applied Chemistry, Chinese Academy of Sciences, Changchun 130022, PR China.
Tel.: +86 431 5262030; fax: +86 431 5698041.
E-mail address: jmeng@ns.ciac.jl.cn (J. Meng).

0925-8388/$ – see front matter
doi:10.1016/j.jallcom.2004.12.198

2. Experimental

A polycrystalline specimen of orthorhombic $BaNd_2Mn_2O_7$ was prepared by the solid state reaction method from the starting materials of Nd_2O_3, $BaCO_3$ and Mn_2O_3. $BaCO_3$ and Mn_2O_3 were used after necessary pretreatment to adjust stoichiometry [17]. Mixtures of $BaCO_3$, Nd_2O_3 and Mn_2O_3 were pressed into pellet, heated at 1423 K for 24 h and subsequently at 1623 K for 72 h in a purified Ar atmosphere, and then very slowly cooled to room temperature. A small excess of Ba-content results into formation of a single phase probably because of a little amount of vaporization of Ba component.

X-ray powder diffraction data of the sample were collected with Cu Kαradiation using MXP[18] X-ray powder diffractometer (MAC Science Co. Ltd.) equipped with a single-crystal graphite monochromator. For data collection 2θ range was $5^\circ \leqq 2\theta \leqq 120^\circ$ with an increment of 0.04° of step width with 4 s per each step [18]. The resulting data were analyzed by Rietveld method using RIETAN program [19,20]. High temperature X-ray diffractometry was used with the same apparatus equipped with high temperature stage under He atmosphere.

3. Results and discussion

The powder X-ray diffraction pattern of $BaNd_2Mn_2O_7$ obtained in this experiment showed that the most probable space group for $BaNd_2Mn_2O_7$ estimated by the CELL program [21,22] belonged to orthorhombic symmetry. The model of the structure for the Rietveld refinement was built according to the previous results [17]. Although a random distribution model for alkaline earth and rare earth atoms over A-site were assumed in the previous analysis [17], where a virtual atom of [(1/3)Ba + (2/3)Nd] was used, and a partially ordered model was used for an analysis of the crystal structure of $Sr_2HoMn_2O_7$ and $Sr_2YMn_2O_7$ [23] in tetragonal $P4_2/mnm$ where [Sr/Ho1]and [Sr/Ho2] and [Sr] and [Sr/Y] are assumed, respectively, an ordering model for Ba in 4b and for Nd in 8i in *Fmmm* space group and also for Ba in 2b and for Nd in 4e in *I*4/*mmm* space group were adopted, respectively, since the results of structure analysis of a single crystal of $BaGd_2Mn_2O_7$ [24] and $BaEu_2Mn_2O_7$ [25] with the tetragonal $P4_2/mnm$ space group gave the ordered distribution of these atoms over A-site. But the difference of the results when a random and an ordered distribution models were used was very slight in the analysis of powdered samples. No other superlattice lines in addition to *Fmmm* phase were observed in the X-ray diffraction patterns. Furthermore, although degree of peak split characteristic of orthorhombic phase (*Fmmm*) from fundamental tetragonal peaks (*I*4/*mmm*) is so small to judge, the results of Rietveld analysis showed a clear difference between these two phases. In this case, *s*-factor is especially a better measure than R_{wp} to judge which phase is more stable in high temperature X-ray diffractometry, where $s = R_{wp}/R_e$ and *s* is a goodness of fit indicator, R_{wp} is a weighted pattern *R*-factor and R_e is an expected *R*-factor. The nearer to unity s is, the more probable space group and the more stable phase at each temperature.

Table 1
Crystallographic data of $BaNd_2Mn_2O_7$ at various temperatures

	rt (*Fmmm*)	473 (*Fmmm*)	523 (*I*4/*mmm*)	773 (*I*4/*mmm*)
a (nm)	0.5486(5)	0.5513(1)	0.3899(0)	0.3903(4)
b (nm)	0.5506(3)	0.5514(9)	–	–
c (nm)	2.0586(7)	2.0610(2)	2.0610(3)	2.0603(1)
V (nm^3)	0.62193	0.62664	0.313322	0.31393
R_{wp} (%)	15.17	13.59	13.59	13.38
R_e (%)	7.07	7.06	7.06	7.06
R_p (%)	12.28	10.51	10.53	10.31
R_i (%)	4.32	4.13	4.08	4.08
R_f (%)	3.4	3.82	3.84	3.97
s	2.15	1.92	1.92	1.89
Ba				
x	0	0	0	0
y	0	0	0	0
z	0.5	0.5	0.5	0.5
B (nm^2)	0.005(2)	0.030(2)	0.030(3)	0.031(3)
Nd				
x	0	0	0	0
y	0	0	0	0
z	0.3152(3)	0.3152(2)	0.3152(3)	0.3151(3)
B (nm^2)	0.012(2)	0.027(1)	0.027(2)	0.028(2)
Mn				
x	0	0	0	0
y	0	0	0	0
z	0.0986(8)	0.0987(7)	0.0987(9)	0.0987(8)
B (nm^2)	0.010(3)	0.025(3)	0.025(3)	0.023(3)
O1				
x	0	0	0	0
y	0	0	0	0
z	0	0	0	0
B (nm^2)	0.00(2)	0.03(2)	0.03(2)	0.03(2)
O2				
x	0	0	0	0
y	0	0	0	0
z	0.203(4)	0.201(4)	0.201(5)	0.198(5)
B (nm^2)	0.01(3)	0.14(3)	0.14(4)	0.14(3)
O3				
x	−0.25	−0.25	0	0
y	0.25	0.25	0.5	0.5
z	0.106(2)	0.105(2)	0.105(2)	0.103(2)
B (nm^2)	0.00(1)	0.042(9)	0.04(1)	0.04(1)

The crystallographic data of orthorhombic at low temperature and tetragonal phases at high temperatures are given in Table 1, respectively, where only several data near the transition temperature and at the highest temperature measured in this study are shown in addition to room temperature. The *s*-factors for orthorhombic (*Fmmm*) and tetragonal (*I*4/*mmm*) phases are shown in Fig. 1 as a function of temperature. It is derived from this figure that the orthorhombic phase is more stable than tetragonal below 523 K, above which temperature the *s*-factor becomes almost same even if either phase is assumed. Therefore, this means that a tetragonal phase exists

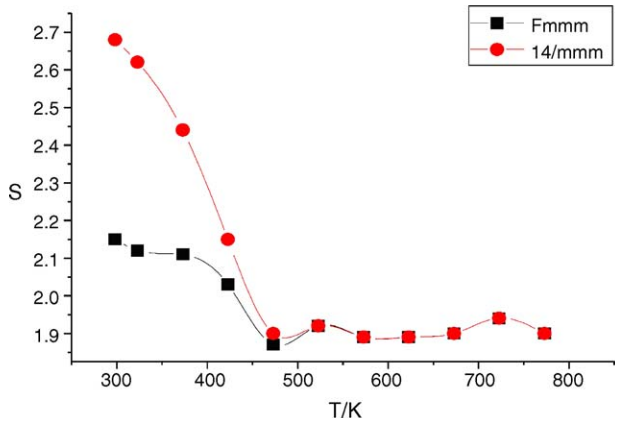

Fig. 1. *s*-Factors for both phases (*Fmmm* and *I*4/*mmm*) as a function of temperature.

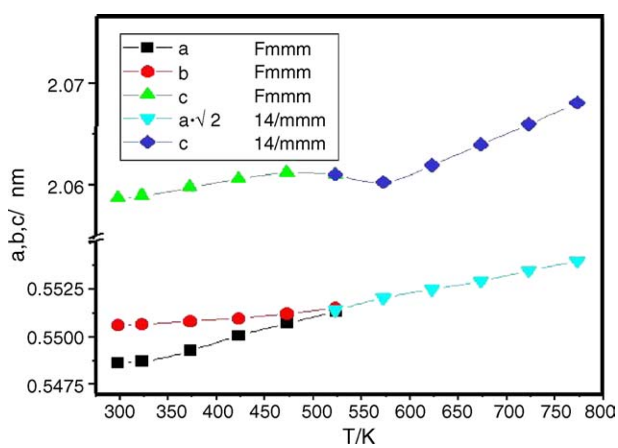

Fig. 2. Variation of the lattice parameters of $BaNd_2Mn_2O_7$ with temperature.

above the transition temperature because of no necessity to lower the symmetry of the crystal. A variation of the lattice parameters with temperature is shown in Fig. 2, where *a* and *b* become united and *c* also changes the dependence near 523 K.

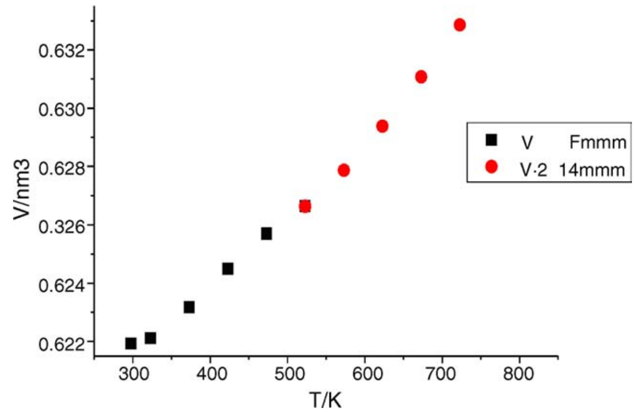

Fig. 3. Temperature dependence of the volume of the unit cell of $BaNd_2Mn_2O_7$.

The temperature dependence of the volume of the unit cell is shown in Fig. 3 where the thermal expansion coefficient has a small knick near the transition temperature.

The bond length and angles of $BaNd_2Mn_2O_7$ are shown in Table 2 at room temperature (*Fmmm*) and at 773 K (*I*4/*mmm*). The corresponding pictures of arrangement of oxygen octahedron in each phase are shown in Fig. 4 at room temperature and at 773 K, respectively. The essential difference between these two phases is shown in Fig. 5, where four O3 atoms forms a rectangle in *Fmmm* and a regular square in *I*4/*mmm* on the plane perpendicular to *c*-axis, respectively. It is concluded from these figures that the nature of the phase transition is a change of quadrilateral consisting of four O3 atoms on the perpendicular to *c*-axis within each oxygen octahedron from a rectangle at low temperature to a regular square at high temperature.

It is also seen from this figure that a manganese atom in the center of each oxygen octahedron are not located on the strict center of four O3 rectangle, but a little apart from this plane and approaches nearer to neighboring manganese atom along *c*-axis. So each oxygen octahedron consisting of the skeleton

Table 2
Bond length (nm) and angles (°) of $BaNd_2Mn_2O_7$ at various temperatures

	rt (*Fmmm*)	473 (*Fmmm*)	523 (*I*4/*mmm*)	773 (*I*4/*mmm*)
Bond lengths (nm)				
Ba—O1 × 4	0.2753(1)	0.2756(1)	0.2757(5)	0.2769(9)
Ba—O3 × 8	0.292(3)	0.291(3)	0.291(3)	0.293(3)
Nd—O2 × 4	0.278(1)	0.278(1)	0.278(1)	0.280(1)
Nd—O2	0.232(8)	0.233(8)	0.234(8)	0.234(9)
Nd—O3 × 4	0.254(3)	0.255(2)	0.255(2)	0.255(3)
Mn—O1	0.203(2)	0.203(1)	0.204(1)	0.205(2)
Mn—O2	0.214(8)	0.213(8)	0.212(8)	0.214(9)
Mn—O3 × 4	0.1949(4)	0.1952(3)	0.1954(3)	0.1963(3)
Ba—Nd	0.3804(6)	0.3807(5)	0.3808(6)	0.3815(6)
Bond angles (°)				
O1—Mn—O3	94(1)	94(1)	94(1)	94(1)
O2—Mn—O3	86(1)	86(1)	86(1)	86(1)
O3—Mn—O3	89.5(2), 89.9(2)	89.7(2), 89.8(2)	89.8(2)	89.8(2)
Mn—O3—Mn	171(3)	173(2)	173(2)	173(3)
Mn—O1—Mn	180	180	180	180

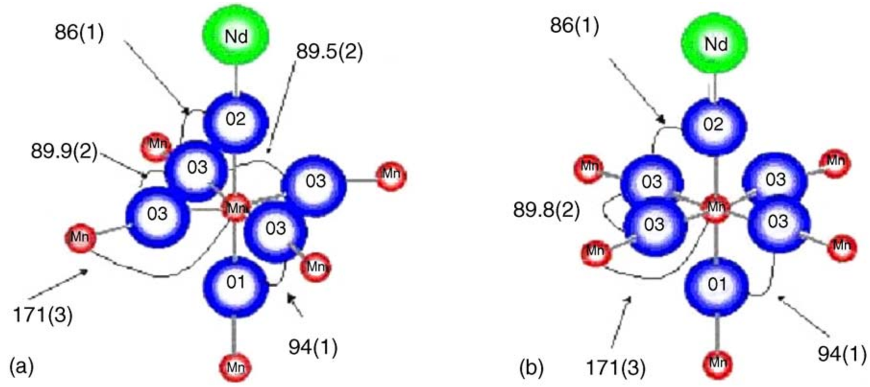

Fig. 4. Environment around a central Mn in each octahedron of $BaNd_2Mn_2O_7$: (a) *Fmmm* at room temperature and (b) *I*4/*mmm* at 773 K.

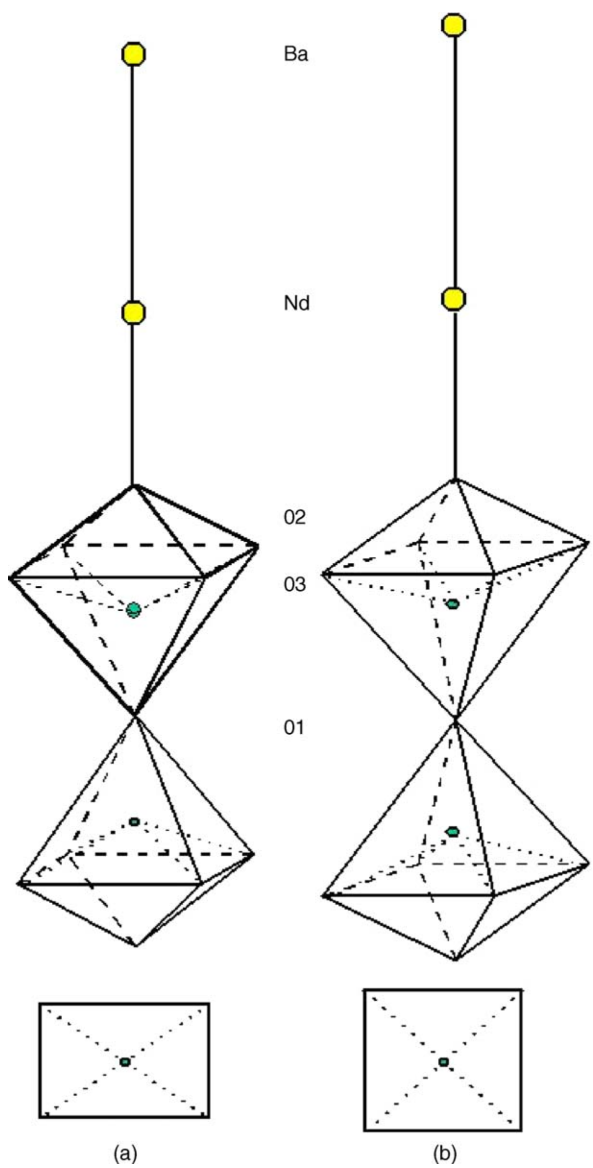

Fig. 5. Cross sections of quadrilateral consisting of four O3 atoms in an octahedron of $BaNd_2Mn_2O_7$ for: (a) *Fmmm* and (b) *I*4/*mmm*.

of this layered perovskite is a little deformed and elongated along *c*-axis in each phase.

Acknowledgement

This work was supported by the Grant-in-Aid for Scientific Research (B) (No. 13450259) by the Japan Society for the Promotion of Science.

References

[1] S.N. Ruddlesden, P. Popper, Acta Crystallogr. 11 (1958) 54–55.
[2] M.N. Deschizeaux-Cheruy, J.C. Joubert, J. Solid State Chem. 40 (1981) 14–19.
[3] N. Kamegashira, S. Umeno, Mater. Chem. Phys. 16 (1986) 89–98.
[4] N. Kamegashira, A. Shimono, M. Horikawa, Mater. Chem. Phys. 24 (1990) 389–397.
[5] N. Kamegashira, Jpn. J. Catal. 31 (1989) 222–226.
[6] N. Kamegashira, S. Umeno, Jpn. J. Appl. Phys. 25 (1986) 238–239.
[7] N. Kamegashira, S. Umeno, Mater. Lett. 4 (1986) 236–238.
[8] N. Kamegashira, M. Icikawa, S. Umeno, M. Aoki, Mater. Chem. Phys. 17 (1987) 585–590.
[9] N. Kamegashira, S. Umeno, H. Satoh, M. Horikawa, Mater. Chem. Phys. 24 (1989) 83–88.
[10] A. Shimono, N. Kamegashira, Mater. Chem. Phys. 21 (1989) 307–311.
[11] A. Shimono, K. Hayashi, N. Kamegashira, Mater. Chem. Phys. 28 (1991) 175–190.
[12] N. Kamegashira, H. Satoh, M. Horikawa, Mater. Lett. 10 (1991) 494–496.
[13] H. Satoh, M. Horikawa, N. Kamegashira, J. Alloys Compd. 192 (1993) 99–101.
[14] H. Satoh, M. Horikawa, N. Kamegashira, Netsu Sokutei 20 (1993) 193–197.
[15] J. Meng, J. Wang, J. Peng, H. Satoh, N. Kamegashira, in: S.H. Feng, J.S. Chen (Eds.), Frontiers of Solid State Chemistry, World Scientific, 2002, pp. 159–165.
[16] N. Kamegashira, J. Meng, T. Mikami, H. Satoh, N. Kakuta, K. Fujita, J. Rare Earths 22 (2003) 17–21.
[17] S. Ueno, N. Kamegashira, Powder Diffr. 12 (1997) 103–105.

[18] T. Horikubi, T. Mori, H. Nonobe, N. Kamegashira, J. Alloys Compd. 289 (1999) 42–47.
[19] F. Izumi, J. Crystallogr. Soc. Jpn. 27 (1985) 23–31.
[20] F. Izumi, J. Mineral. Soc. Jpn. 17 (1985) 37–50.
[21] Y. Takaki, T. Taniguchi, K. Nakata, H. Yamaguchi, J. Ceram. Soc. Jpn. 97 (1989) 763–766.
[22] Y. Takaki, T. Taniguchi, K. Hori, J. Ceram. Soc. Jpn. 101 (1993) 373–376.
[23] P.D. Battle, J.E. Mullburn, M.J. Rosseinsky, L.E. Spring, J.F. Vente, Chem. Mater. 9 (1997) 3136–3143.
[24] N. Kamegashira, J. Meng, T. Mori, A. Murase, H. Satoh, T. Shishido, T. Fukuda, Mater. Lett. 57 (2003) 1941–1944.
[25] N. Kamegashira, J. Meng, T. Murase, K. Fujita, H. Satoh, T. Shishido, T. Fukuda, in: P. Vincenzini (Ed.), Proceedings of CIMTEC 2002 – 10th International Ceramics Congress and 3rd Forum on New Materials, Techna Srl, 2003, ISBN: 88-86538-32-4.